www.sciencemag.org/content/348/6235/694/suppl/DC1

Supplementary Materials for

Long-term measles-induced immunomodulation increases overall childhood infectious disease mortality

Michael J. Mina,* C. Jessica E. Metcalf, Rik L. de Swart, A. D. M. E. Osterhaus, Bryan T. Grenfell

*Corresponding author. E-mail: michael.j.mina@gmail.com

Published 8 May 2015, *Science* **348**, 694 (2015)
DOI: 10.1126/science.aaa3662

This PDF file includes:

Other Supplementary Materials for this manuscript include the following:
(available at www.sciencemag.org/content/348/6235/694/suppl/DC1)

Materials and Methods

MATERIALS AND METHODS

1. DATA SOURCES AND PREPARATION

A. England & Wales

Measles data

Age- and gender-structured quarterly measles virus (MV) incidence data for E&W came from the *Annual Reviews of the Registrar General of England and Wales* and the *Statistics of Infectious Diseases* published by the Office of Population Censuses and Surveys (OPCS), as described in Anderson and Grenfell (*41*).

Non-measles infectious disease mortality

Age- and gender-structured mortality data were collected from the Office for National Statistics (ONS; http://www.ons.gov.uk/ons/datasets-and-tables/index.html). The datasets can be found by searching for "The 20th Century Mortality Files". See Table S1 (column headers) for specific names of each data set used. Mortality data was listed as yearly totals for each age and gender by ICD codes specific for each respective ICD era (5, 6, 7, or 8; see Table S1). Codes used to create the 'non-measles infectious diseases mortality' data are listed in Table S1.

To specifically observe associations between measles and non-measles mortality that would be affected by underlying changes in acquired immunity, four basic criteria for inclusion of a cause of death in our analysis were required to be met. The infectious cause has to:

- Generally present as an acute (rather than chronic) infection,
- Be present at a common enough frequency such that development of acquired immunity would be expected within the population (which we defined as greater than one death in each year of the analysis),
- Is not the result of an infection recorded as food poisoning or a bite from an animal
- Is not a vaccine preventable cause of death (as inclusion could bias results toward an association between measles and mortality).

These exclusions had no qualitative (and very little quantitative) effect on the results and conclusions presented.

Population data

Annual age- and gender-stratified population data were also collected from ONS and can be found by searching for "The 20th Century Mortality Files – Populations 1901-2000".

B. United States

Measles data

Age- and gender-structured annual measles mortality incidence data were collected from source documents accessible from National Center for Health Statistics (NCHS), housed within the US Centers for Disease Control and Prevention (CDC) and can be located online at (http://www.cdc.gov/nchs/nvss/mortality/hist290.htm).

Age- and gender-stratified measles incidence rates were reconstructed using annual measles mortality rates previously published by the CDC (*42*). We ensured this method captured the true annual measles dynamics by comparing the reconstructed data, after summing over all age strata, to unstratified measles data previously published for the entire US population for each year of interest (*42*). No important differences existed (pearson correlation coefficient = .94).

Yearly measles incidence data was further partitioned into quarterly (3 month) incidence data. To most accurately accomplish this, we collected weekly surveillance data from all 50 states from each year of analysis using only level 1 (the highest quality) data within the Project Tycho® database (see (*43*) for details). We then summed the numbers of cases within each quarter of each year over all 50 states, and from this calculated proportions of measles cases for the whole of the US for each 3-month period, relative to the respective annual sum. The yearly measles incidence data was then partitioned into quarterly data by multiplying each datum across the proportions calculated within each respective year.

Non-measles infectious disease mortality data

Age- and gender-structured infectious disease mortality data was collected from the same NCHS source documents described above. In these datasets, mortality is grouped by infectious disease class, rather than ICD code. Using the same selection criteria as in the UK, we extracted causes of mortality for analysis, which included: “acute bronchitis & bronchiolitis”, “bronchitis”, “other bronchopulmonic diseases”, “diarrheal diseases”, “dysentery”, “infections and parasitic diseases”, “meningitis”,

"pneumonia (separate from influenza)", "scarlet fever", "pneumococcal sore throat", and "septicemia".

Population data

Age- and gender-structured population data for the US was also collected from the NCHS, as described above.

C. Denmark

Measles data

Measles incidence data for Denmark was collected from the World Health Organization (WHO) vaccine preventable diseases monitoring system (www.apps.who.int). For the secondary analysis mentioned in the main text, these yearly data were partitioned into quarterly intervals by assigning specific proportions of the yearly incidence into their respective months, based on data describing the monthly proportion of annual measles cases in Denmark (*33*).

Non-measles infectious disease mortality data

Age- and gender-structured mortality data came from the Denmark national statistics registry (Statistics Denmark: www.statbank.dk), which contains deaths by sex, age and cause of death. Similar to the US data, causes of death were grouped together, so we used all infectious causes of diseases that fit the criteria as specified for the E&W data. Categories used were: "acute respiratory infections", "infective and parasitic diseases", "meningitis" and "pneumonia".

Population data

Age- and gender-structured population data was also retrieved from Statistics Denmark.

2. TRANSFORMATION OF MEASLES INCIDENCE TO PREVALENCE OF MEASLES-INDUCED IMMUNOMODULATION

We transformed measles incidence data into 1-year period prevalence of immunomodulation by applying either of two distinct transformations (as mentioned in the text): i) a simple additive function or ii) a gamma distributed function to the measles incidence data, to derive the number of individuals with immunomodulation (i.e., with immune memory loss that has not yet been fully regained) during each 3-month (or 1-year for Denmark) interval (described below), and then converted from total numbers of individuals with immunomodulation within each interval to 1-year period prevalence as described below. Illustrations of the transformation from measles incidence data to measles immunomodulation data, using both the additive and gamma transformations are depicted in Figure S1 and Movie S1.

The distribution of measles cases within a given interval for which the data were collected or prepared (i.e. 3-months for the E&W and US data, plus a sub-analysis of the Denmark data and 1-year for the Denmark data – see text) was assumed uniform, and the shortest duration of immunomodulation possible was equal to the length of the interval. Thus, on average, half of the burden of immunomodulation developed as a result of MV infections in a given interval would

reside within the succeeding interval. Therefore, we first processed the data by shifting half of the burden of measles cases from the quarter or interval in which they were recorded to the succeeding interval. To account for changes in age class (and assuming uniform distribution of measles cases within age classes) a fraction of the shifted burden (defined as: $\frac{length\ of\ interval\ (L_i)}{length\ of\ age\ class\ (L_z)}$) was also shifted to the next age class. Thus, for age group (z) and interval (i), the number (n) of measles incident cases is:

$$n_{z_i} = \frac{1}{2}\left(n_{z_i} + n_{z_{i-1}} \cdot \left(1 - \frac{L_i}{L_z}\right) + n_{(z-1)_{i-1}} \cdot \left(\frac{L_i}{L_{z-1}}\right)\right) \qquad \text{Eq. (1)}$$

The details of this initial transformation had no qualitative effects on any of the results, and very little quantitative effects, however we felt this initial processing step was important to best represent the prevalence of measles-induced immunomodulation over time.

Both transformations were based on applying a cumulative lag such that the full (additive), or partial (gamma) numbers of measles cases from previous intervals persist and contribute to the numerator of the rate of individuals with measles-induced immunomodulation for the interval of interest (see Fig. S1 and Movie S1). The additive transformation, for example, sums together the current interval of interest, plus contiguous preceding intervals. The number of intervals summed together times the length of each interval thus represents the duration of immunomodulation for the additive transform. As a simple example of the additive transform (and if we ignore age class for a moment), if the duration of

immunomodulation is considered to last for 9 months, then the number of individuals with immunomodulation (N) within a given quarter (i) would be the combined cases from the quarter of interest plus the previous two quarters: $N_i = n_i + n_{i-1} + n_{i-2}$.

For both transformations, as the duration of immunomodulation is extended from its known baseline of 3 months, the incident cases from each interval move through age classes. Thus, similar to Eq. (1) above, as time increases and previous measles incident cases are carried to more recent intervals, for each interval carried forward, a fraction of the incident cases $\left(\frac{L_i}{L_z}\right)$ are simultaneously moved to the ($z + 1$) age class and, later, to the $z + 2$ age class, $z + 3$, etc… depending on the duration of immunomodulation (Fig S1 and Movie S1 illustrate this process). Further, because MV incidence within age classes was assumed uniform, any age classes with a duration greater than one year were uniformly partitioned into one-year classes (i.e. 0-1, 1-2, 2-3, etc…) in order to simplify calculations by making $\left(\frac{L_i}{L_z}\right)$ into a constant $\left(\frac{1}{4}\right)$.

Both transformations, the additive and the gamma transform, take similar forms, but differ based on a controlling parameter $\boldsymbol{\delta}$, which directly controls the duration of immune suppression. The transformed value (N_{Z_i}) for the number of individuals with immunomodulation for a given age class, z, and interval i, and given a duration of immunomodulation (described by $\boldsymbol{\delta}$) can be calculated directly from equation 2 (depicted in Fig. S1 and Movie S1):

$$
\mathrm{N}_{Z_i}\,|\{\delta, m\}
$$

$$
= \begin{cases} n_{z_i} \cdot \delta_{[1]} + \sum_{k=i-1}^{k=i-4} \left[\left(1 - \frac{i-k}{4}\right) \cdot \sum_{j=0}^{j=m} n_{(z-j)_{[k-4j]}} \cdot \delta_{[i-k+(4_j+1)]} \right] & : m = 0 \\ n_{z_i} \cdot \delta_{[1]} + \sum_{k=i-1}^{k=i-4} \left[\left(\left(1 - \frac{i-k}{4}\right) \cdot \sum_{j=0}^{j=m} n_{(z-j)_{[k-4j]}} \cdot \delta_{[i-k+(4_j+1)]} \right) + \left(\left(\frac{i-k}{4}\right) \cdot \sum_{j=1}^{j=m} n_{(z-j)_{[k-(4j-4)]}} \cdot \delta_{[i-k+(4_j-3)]} \right) \right] & : m > 0 \end{cases} \qquad \text{Eq. (2)}
$$

Here, i refers to the absolute interval, such that the first interval of the time series is i =1, the second interval is 2 and so on. $\boldsymbol{\delta}$ is a row vector of length d, where d is the number of preceding intervals, plus the i^{th} that contribute to N_i, and each element of $\boldsymbol{\delta} \in [\delta_1, \delta_2, \delta_3, \dots, \delta_d]$ describes the proportion that the respective interval ($\in [i, i-1, i-2, \dots, i-d+1]$) contributes to N_i. In other words, $\boldsymbol{\delta}$ is a vector of weights describing the contributions of each of the d intervals. Thus, each element of $\boldsymbol{\delta}$ is a value between 0 and 1, inclusive, and for reasons that will become evident, its length (d) must be a multiple of 4 (but this does not mean that the durations of immunomodulation must be multiples of 4).

The parameter m in Eq. 2 takes on a non-negative integer value equal to $\frac{d}{4} - 1$ and represents the number of years, beyond the incident year, for which some level of immunomodulation (including 0% if using the additive transformation), persists following measles. Thus, values of m of: 0, 1, 2 or 3 represent inclusion of: 1, 2, 3 or 4 years of previous measles cases to the interval of interest or, equivalently,

$d = 4, 8, 12,$ or 16 intervals contributing to N_i (assuming 3-month durations for each interval).

Thus, while m (or d) dictates the number of years (or intervals) that potentially contribute in some way to N_i, $\boldsymbol{\delta}$ indicates the proportion of each of those intervals that is ultimately contributed (including 0%). The values that populate $\boldsymbol{\delta}$ comprise *the* distinguishing feature between the additive and gamma transformations. (Note that for clarity of illustration in figure S1 and movie S1, we did not include all of the *d* intervals that contribute 0% of their measles cases to the interval of interest.)

A. Additive transformation

For the additive transformation, each element of $\boldsymbol{\delta}$ takes on only values of 1 or 0, meaning that each of the d intervals either contributes entirely or not at all to N_i. The first element of $\boldsymbol{\delta}$ should be a 1, indicating that 100% of the cases within the i^{th} interval (n_i) contribute to the number with immunomodulation within that same interval (N_i). Following the first element of $\boldsymbol{\delta}$, elements 2 through d must be contiguous 1's or 0's (1's must always precede 0's). The total number of contiguous 1's (including the first element) is the number of intervals for which immunomodulation persists $\left(\text{ie: } \frac{\text{duration (months) of immunomodulation}}{\text{3 months}}\right)$. Thus, for the additive transform, duration of immunomodulation must be a multiple of 3 months. For example if 8 intervals contribute to the number with immunomodulation ($d = 8$) in the i^{th} quarter (N_i), and the immunomodulation lasts for 9 months, then $\boldsymbol{\delta}$ in Eq. 2 would be $[1, 1, 1, 0, 0, 0, 0, 0]$. Thus, using this example, if age structure were

neglected (as it is with the yearly Denmark measles data), then to transform MV incidence data ($\boldsymbol{n_i}$), into total numbers of individuals with immunomodulation (N_i): $\boldsymbol{\delta} = (1\ \ 1\ \ 1\ \ 0\ \ 0\ \ 0\ \ 0\ \ 0)$ and

$$N_i = \boldsymbol{n_i}\boldsymbol{\delta}^{\boldsymbol{T}} \qquad \text{Eq. (3)}$$

where : $\boldsymbol{n_i} = (n_i \quad n_{i-1} \quad n_{i-2} \quad n_{i-3} \quad n_{i-4} \quad \dots \quad n_{i-d+1})$.

B. Gamma transformation

For the gamma transformation, $\boldsymbol{\delta}$ is drawn from the survivor function (S) of the cumulative gamma distribution function (Γ_{cdf}). This is depicted in figure S1(c-ii-iii). Eq. 4 shows the form of the survivor function, S:

$$S(x, \alpha, \gamma) = 1 - \Gamma_{cdf}(x|\alpha, \gamma) \qquad \text{Eq. (4)}$$

where α and γ are the shape and rate parameters that control the gamma probability distribution, and x represents time in months since measles infection. The cumulative gamma distribution function takes the form:

$$\Gamma_{cdf}(x|\alpha, \gamma) = \frac{\gamma^{\alpha}}{\Gamma(\alpha)} \int_0^x t^{\alpha-1} \cdot e^{-\gamma t}\, dt \qquad \text{Eq. (5)}$$

where $\Gamma(\alpha)$ is the gamma function:

$$\Gamma(\alpha) = \int_0^{\infty} t^{\alpha-1} \cdot e^{-t}\, dt = (\alpha - 1)! \qquad \text{Eq. (6)}$$

(the latter simplification in Eq. (6) is appropriate for all α that are positive real integers). When used to populate $\boldsymbol{\delta}$, x is a row vector ($\boldsymbol{x}$) of length d where:

$\boldsymbol{x} = [3, 6, 9, \dots, 3d]$ indicates an index of each interval (i to $i - d + 1$) that contributes to N_i. Thus, $S(x, \alpha, \gamma)$ represents the probability that an individual will

remain in an immunomodulated state at x months after measles infection or, alternatively, the proportion of individuals in the $(i - \frac{x}{3} + 1)^{th}$ interval with immunomodulation contributing to N_i. Thus, for the gamma transformation:

$$\boldsymbol{\delta} = S(\boldsymbol{x}, \alpha, \gamma) \qquad \text{Eq. (7)}$$

and, similar to the additive transform, if age class were ignored then:

$$N_i = \boldsymbol{n_i}\boldsymbol{\delta^T} = \boldsymbol{n_i} \cdot S(\boldsymbol{x}, \alpha, \gamma)^T \qquad \text{Eq. (8)}$$

and: $\boldsymbol{n_i} = (n_i \quad n_{i-1} \quad n_{i-2} \quad n_{i-3} \quad n_{i-4} \quad \dots \quad n_{i-d+1})$.

Although the intervals remain in 3-month segments, using the gamma distribution essentially changes the nature of the transformation from a cumulative step function (as it is for the additive transform above) to a continuous transformation. This is evident, for example, by inspection of the survival curve, $S(\alpha, \gamma)$, that resulted in the best-fit transformation for the E&W data – shown in Fig. 2g, where $\alpha = 35$ and $\gamma = 1.236$. The curve itself shows the distribution of proportions in an immunomodulated state as a continuous function over time since measles infection – and $\boldsymbol{\delta}$ takes on the values of the curve at $\boldsymbol{x} = [3, 6, 9, \dots, 3d]$ months. For reporting purposes, we considered the time at which $S(\alpha, \gamma) = 0.5$ to be the mean duration of immunomodulation for a particular transformation (28.3 months for the best-fit transformation shown in Fig 2), as this represents the time post-measles for a given α, γ combination where 50% of individuals are considered 'recovered' from the immunomodulatory effects of immune memory loss. Estimation of the mean duration of immunomodulation for any α, γ pair is straight forward, as the mean of

$S(\alpha, \gamma)$ (i.e. x for which $S(x, \alpha, \gamma) = 0.5$) is simply $\frac{\alpha}{\gamma}$ (e.g. $\frac{\alpha}{\gamma} = \frac{35}{1.236} = 28.3$ months). In practice however, we used the quantile function of the gamma distribution (*qgamma*) available in the base R statistical language (see below) to calculate the mean centered duration and 1-the cumulative gamma distribution function (1-pgamma($\boldsymbol{x}, \alpha, \gamma$); also available in base R) to calculate $\boldsymbol{\delta}$.

C. Setting the parameters d and m.

It was important to set d (the number of intervals that contribute some fraction of MV cases – even zero - to N_i) and thus m (the equivalent number of years to include) as conservatively as possible, while still ensuring to capture the best-fits, because the first calculable N_i from the beginning of the time series is the d^{th} interval ($N_{i=d}$) as any N_i for $i < d$ would be incomplete. For example if d = 4 (representing a maximum immunomodulation of 12 months), calculation of $N_{i=2}$, would be missing the contributions from the 2 intervals just prior to the start of the time series.

For all transformations reported, we set d = 16 (and thus $m = 3$), as the proportions with immunomodulation at 48 months (d=16 intervals) after measles were negligible for all transformations within the 95% confidence of the best-fit transformations (methods for determining best-fit are described below).

D. Post-transform conversion to immunomodulation

To convert the (transformed) numbers within each age class with immunomodulation in each interval (N_{z_i}) to 1-year period prevalence for fitting against the yearly mortality data, we first summed N_{z_i} across all age groups (z) of

interest (e.g. z=1-9) within each interval (i) to get N_i and divided N_i by the total population of interest for the respective interval (populations were assumed constant within a give year) to get interval rates. The 1-year period prevalence for each year was then calculated as the integral of the curve of the interval rates, within each respective year.

3. OPTIMIZING THE BEST-FIT DURATION OF IMMUNOMODULATION

The goodness-of-fit of the transformed measles immunomodulation data was determined by regressing the yearly incidence of non-measles infectious disease mortality against the transformed yearly prevalence of measles-induced immunomodulation (i.e. non-MV mortality = $\beta_o + \beta_1 \cdot$ (MV immunomodulation)), and calculating R^2. Examples of these regressions are the scatter plots shown in Figs. 1, 2 and 3. The best-fit duration of immunomodulation was then optimized by searching for the duration of immunomodulation that provided the highest R^2 value.

A. Optimizing the duration of immunomodulation in different eras and calculating beta-coefficients

As described in the main text, we first optimized the durations of immunomodulation by finding the best-fit using the entire set of years and subsequently, to check for vaccine effects, also optimized these durations over the pre-vaccine years only and post-vaccine years only. For each of these three individual optimized transformations of the data, we also calculated the coefficients of association (β_1) for the full data, the pre-vaccine data and the post-vacccine data

(see Figs. S5 and S9). Thus, in total for each country we derived nine different values for β_1 as shown in Figs. S5 and S9. There was only slight 'intra-transform' variation between the $\beta_1$values. This means that the variation in the $\beta_1$values for the full data set, the pre-vaccine years and the post-vaccine years for a given optimal transformation (i.e., the optimal transformation based off of the full dataset or the optimal transformation based off of only the pre-vaccine data) was minimal. Further, there was virtually no 'between-transform' variation in the each of the respective eras' $\beta_1$values. Effectively, this means there was consistency across the time-series in terms of the optimal duration of immunomodulation and, as well, regardless of the transformation, the effect of measles on non-measles mortality was consistent. Thus, particularly for E&W, where the $\beta_1$coefficients between eras were virtually identical, parameterization using only the pre-vaccine era data can predict out-of-sample the post-vaccine era mortality data almost as well as the post-vaccine era data can perform an in-sample prediction of the same post-vaccine mortality. This was shown by the red line in Figure 2F.

B. Additive Transformation

When using the additive transformation, optimizing the transformation by the highest R^2 was done simply by calculating R^2 for each set of the transformed data as the duration of immunomodulation was increased from 3 months:

$\boldsymbol{\delta} = [1,0,0,0,0,0,0,0,0,0,0,0,0,0,0,0]$

to 48 months:

$\boldsymbol{\delta} = [1,1,1,1,1,1,1,1,1,1,1,1,1,1,1,1]$

(note: $d = 16$ elements) as shown in Figures 2d and 3d. The optimal or best-fit duration of immunomodulation was then identified as the transformation with the highest R^2 value.

C. Gamma Transformation

Determination of the best-fit duration of immunomodulation using the gamma transformation was similar in principle, however it required optimization via a search over the parameter space of both the α and γ parameters of the survival function, S(α, γ). We used an implementation of the Nelder-Mead optimization algorithm, which is standard in the base R statistical environment; to minimize the negative R^2 value of the linear regression of the non-measles mortality against the gamma transformed measles data.

While the best fit reported was based on this Nelder-Mead optimization, the curves displayed in figures 2c and 3c (R^2 versus mean duration of immunomodulation) were derived by holding the best-fit shape parameter (α) constant at its "Nelder-Mead-optimum" and varying the rate parameter (γ). The peak and shape of the curve were consistent regardless of which parameter was held constant.

95% boot-strapped confidence intervals were also calculated (shaded regions in Figs. 1g and 2g) for each parameter while holding the other at its respective optimized value from the Nelder-Mead optimization. This was essential because the shape of the of $\Gamma_{cdf}(\alpha, \gamma)$ curve, and thus the S(α, γ) curve**,** at any particular α is highly dependent on γ, and vice versa. Thus, similar curves could be

generated from values of the parameters spanning logs of either variable's parameter space when the other parameter scaled with it.

4. ADJUSTING FOR YEAR

Because mortality generally trends downwards in time, it was important to ensure our results are not simply an artifact of increasing time causing declines in both measles incidence and all-cause non-measles infectious disease mortality. Thus, as discussed in the main text, we adjusted for year by including it as a covariate in the linear regression used to assess the fit between measles-induced immunomodulation and mortality (i.e. non-MV mortality = $\beta_o + \beta_1 \cdot (\text{MV immunomodulation}) + \beta_2 \cdot \text{year}$).

If year is an important confounder, it would reduce the significance and magnitude of the association between prevalence of measles-induced immunomodulation and mortality, and would itself be a significant predictor of mortality, as discussed in the text. It was not, as discussed and described in Figs. S4 and S12.

5. UNDER-5 YEAR OLD DISTRIBUTION OF INVASIVE BACTERIAL DISEASE

Risk of disease from infectious causes generally increases throughout the first two years of life (described below), in particular following reduction of maternal antibodies. During this period, children are building their immune repertoire through exposure, vaccination and cross-reactive antigen stimulation. When risk of

mortality *begins to decrease* is when children begin to develop a sufficiently diverse complement of protective immunity that is sufficient to reduce morbidity and mortality at the population level.

Therefore, the distribution by age of invasive bacterial disease from common pathogens in under-five year-old children is a good proxy for time required for development of immune memory through exposure, in particular following the period of greatest protection from maternal antibodies –the first 6 months of life.

Given the hypothesis that an ablated immune-memory repertoire (following measles) requires re-exposure to return to fully protective levels (as discussed in the main text), full immunologic recovery from measles should follow a similar temporal pattern to that of initial development of immunity (following depletion of maternal antibodies). Therefore, to compare the best-fit durations of post-measles immunomodulation to development of immunity in early childhood, we collected data from the WHO and developed a global picture of development of immunity, as reflected by the distribution of under-5 year bacterial invasive disease. Data came from 19 countries and included 17,349 cases of disease in under-five year old populations, as described in (*32*). Figure S2a shows the distribution of cases among under 5-year olds for each country and Fig. S2b shows the mean with 95% confidence intervals overlaid. Of note, the period in which prevalence of disease is increasing in the under-five year olds is considered to precede development of full-immunity. Thus, during this period full immunity has not yet developed and is therefore analogous to $S(\alpha, \gamma) = 1$. The mean curve in figure S2b is the same curve that appears as the broken line with confidence bars in Figures 2g, 3g and 4c.

6. OBSERVED RELATIVE RISK OF MORTALITY FOLLOWING MEASLES INFECTIONS

As a further test of our results, we compared the best-fit curve for duration of immunomodulation (which indicates the duration of or recovery from increased risk of mortality following measles) to observed increased rates of mortality following measles infections versus matched measles uninfected children reported by Aaby et al. (see below and (*31*)). Aaby reported probability of survival at approximately 6-18 months, 18-29 months and 30-54 months following measles infections. Thus, we plotted each point at the center of these intervals and relative risk of mortality for MV infected vs. uninfected controls for each interval was calculated as:

$$RR = \frac{1-Probability\ of\ survival\ (MV\ infected)}{1-Probability\ of\ survival(controls)}. \qquad \text{Eq. (9)}$$

These points are the blue dots marked with their respective relative risk in Figures 2g, 3g and 4c.

7. STATISTICAL AND MATHEMATICAL ENVIRONMENT:

All mathematical and statistical work (described above) was performed within the R statistical environment (http://www.R-project.org/) using version R version 3.1.0.

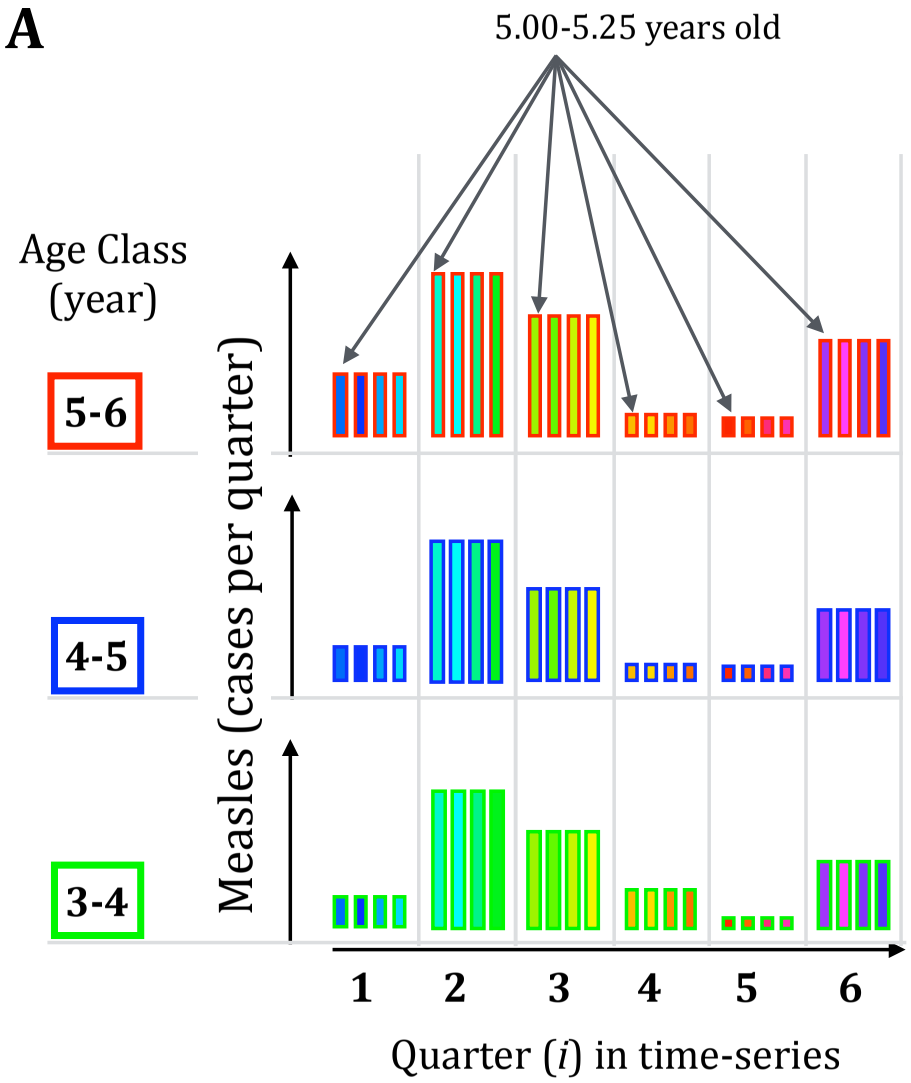

Each column within a given quarter represents the children who were infected with measles during months the first, second, third or fourth quarter of their respective age class.

- The first column of each quarter are children who have been in their respective Age Classes for 1-3 months (0-.25 years).
- The second column represent children who have been in their Age Class for 4-6 months
- 3rd column for 7-9 months
- 4th column for 10-12 months.

Figure S1a: Transformation of the measles incidence data to prevalence of MV immunomodulation data: an illustrated example: Calculate the number of 5-6 year olds with immunomodulation in **quarter 6** of the time series from the **(A)** measles incidence using the **(B)** Additive transformation centered at 18 months duration of immunomodulation and **(C)** the gamma transformation centered at 10 months.

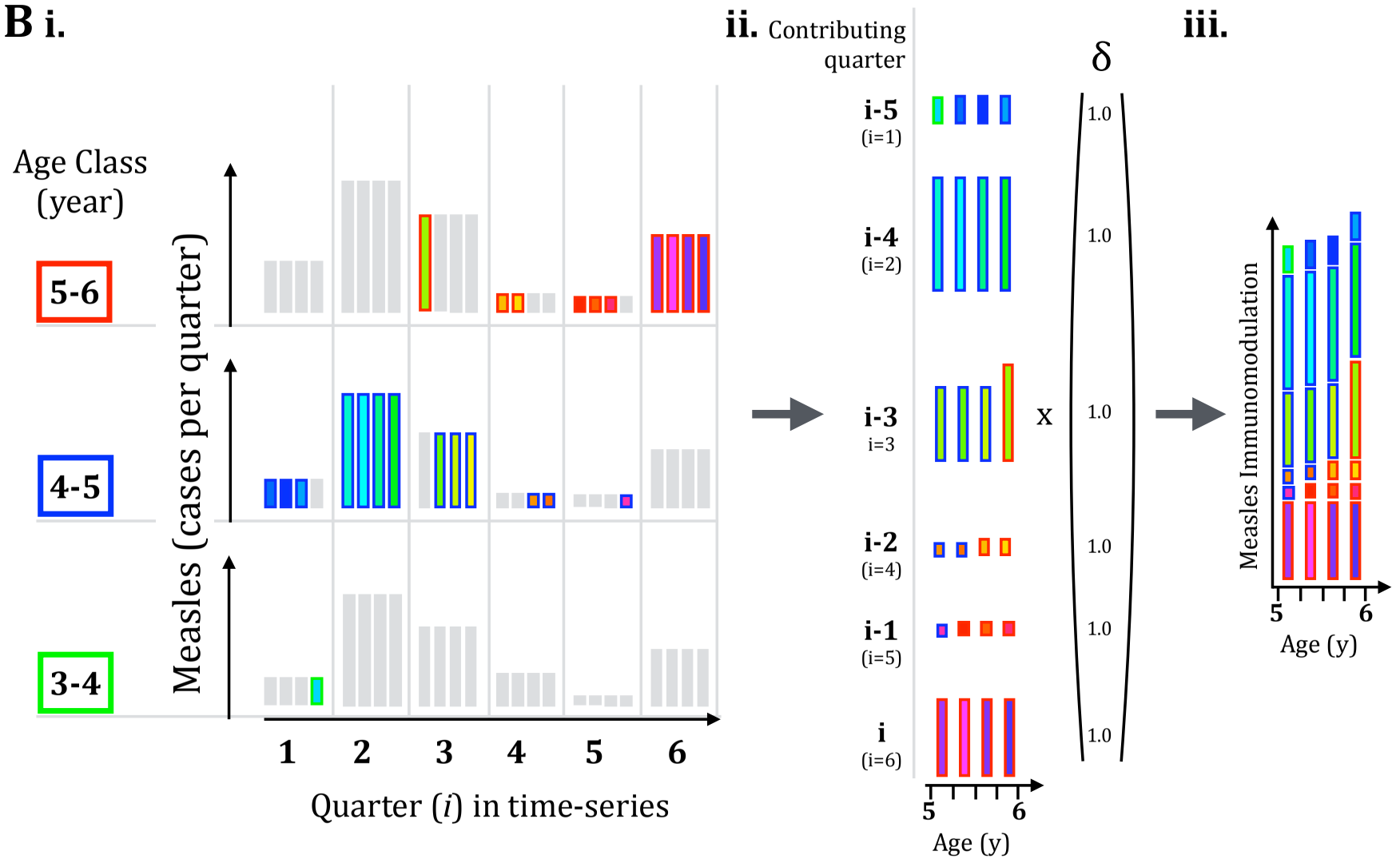

Figure S1b: Transformation of the measles incidence data to prevalence of MV immunomodulation data: an illustrated example: Calculate the number of **5-6 year olds** with MV immunomodulation in **quarter 6** of the time series from the **(A)** measles incidence data **(i)** using the additive transformation and an immunomodulatory effect lasting 18 months. **(ii)** The appropriate numbers of measles infected individuals from earlier quarters and age classes are carried over, multiplied by δ (see SOM methods) and **(iii)** summed together to get the number of 5-6 year olds with immunomodulation during a particular quarter of the time series (here i=6).

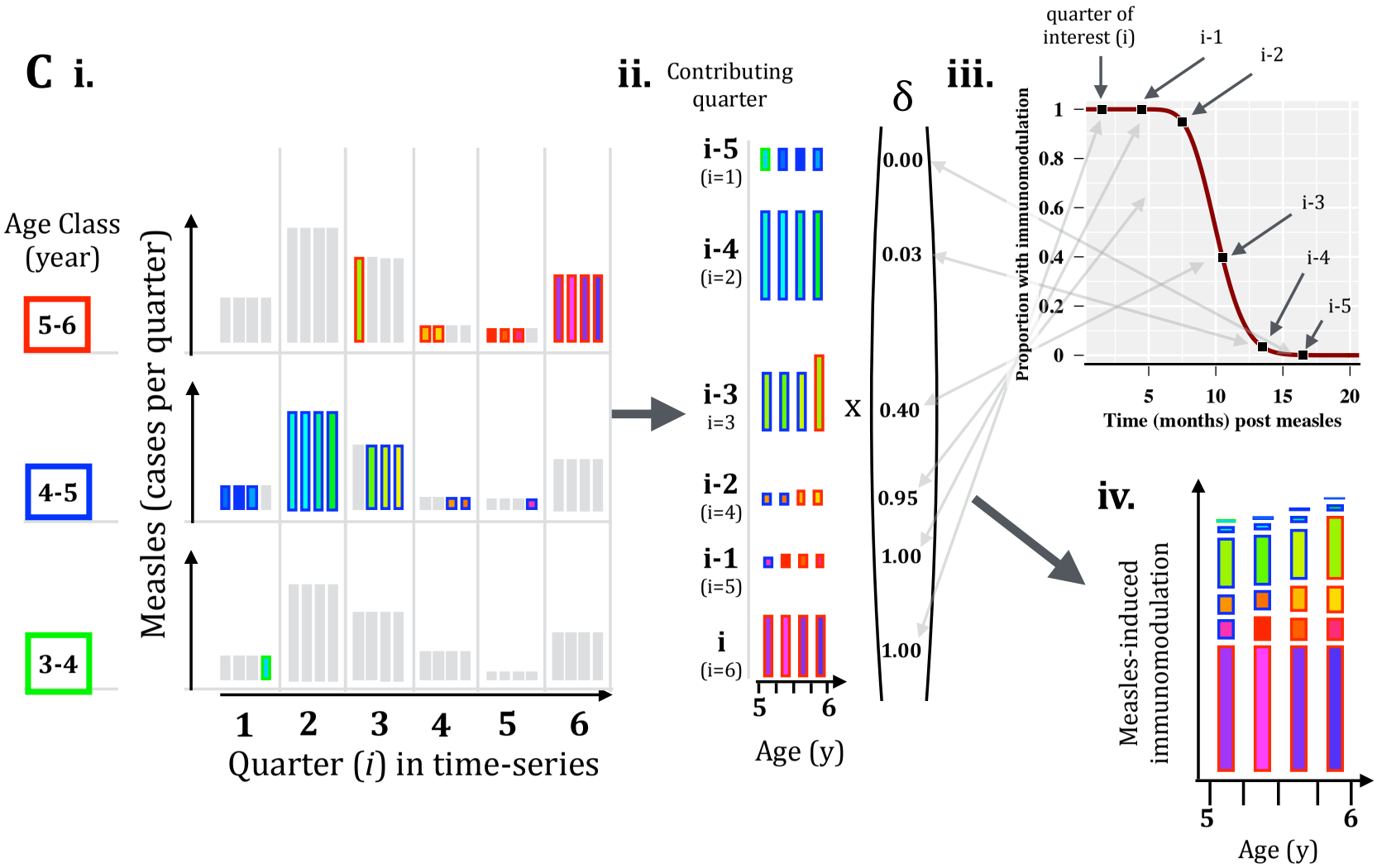

Figure S1c: Transformation of the measles incidence data to prevalence of MV immunomodulation data: an illustrated example: Calculate the number of **5-6 year olds** with MV immunomodulation in **quarter 6** of the time series from the **(A)** measles incidence data **(i)** using the gamma transformation and an MV immunomodulation centered at 10 months. **(ii)** The appropriate numbers of measles infected individuals from earlier quarters and age classes are carried over and multiplied by δ, derived from the **(iii)** gamma curve of interest (see SOM methods), and **(iv)** summed together to get the number of 5-6 year olds with immunomodulation during the 6th quarter of the time series (here i=6).

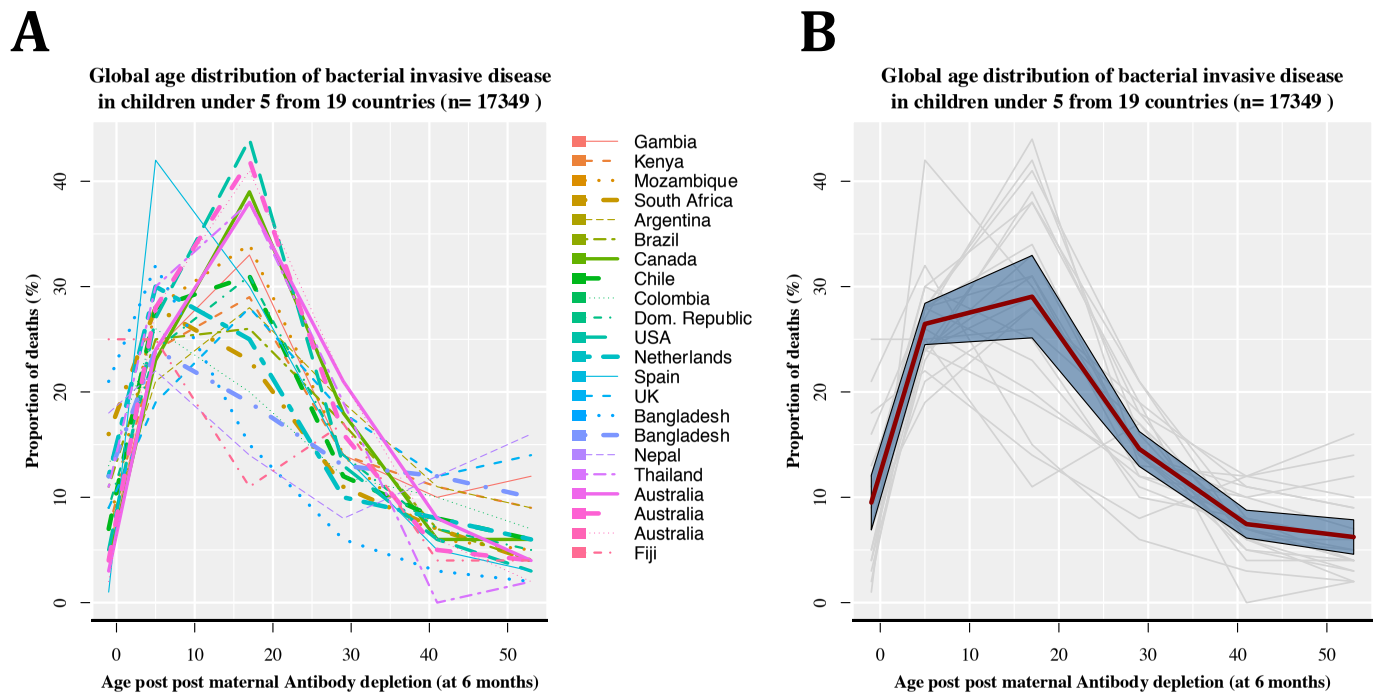

Figure S2: Global age-distribution of bacterial invasive disease in children under 5 years of age. (A) Age distribution stratified by nation in which the study supplying the data took place. **(B)** Mean (red line) and 95% confidence intervals (blue shaded region) for the age-distributions shown in (A) are plotted, overlaying the individual curves seen in (A). Data is from the WHO, as described in the SOM methods section.

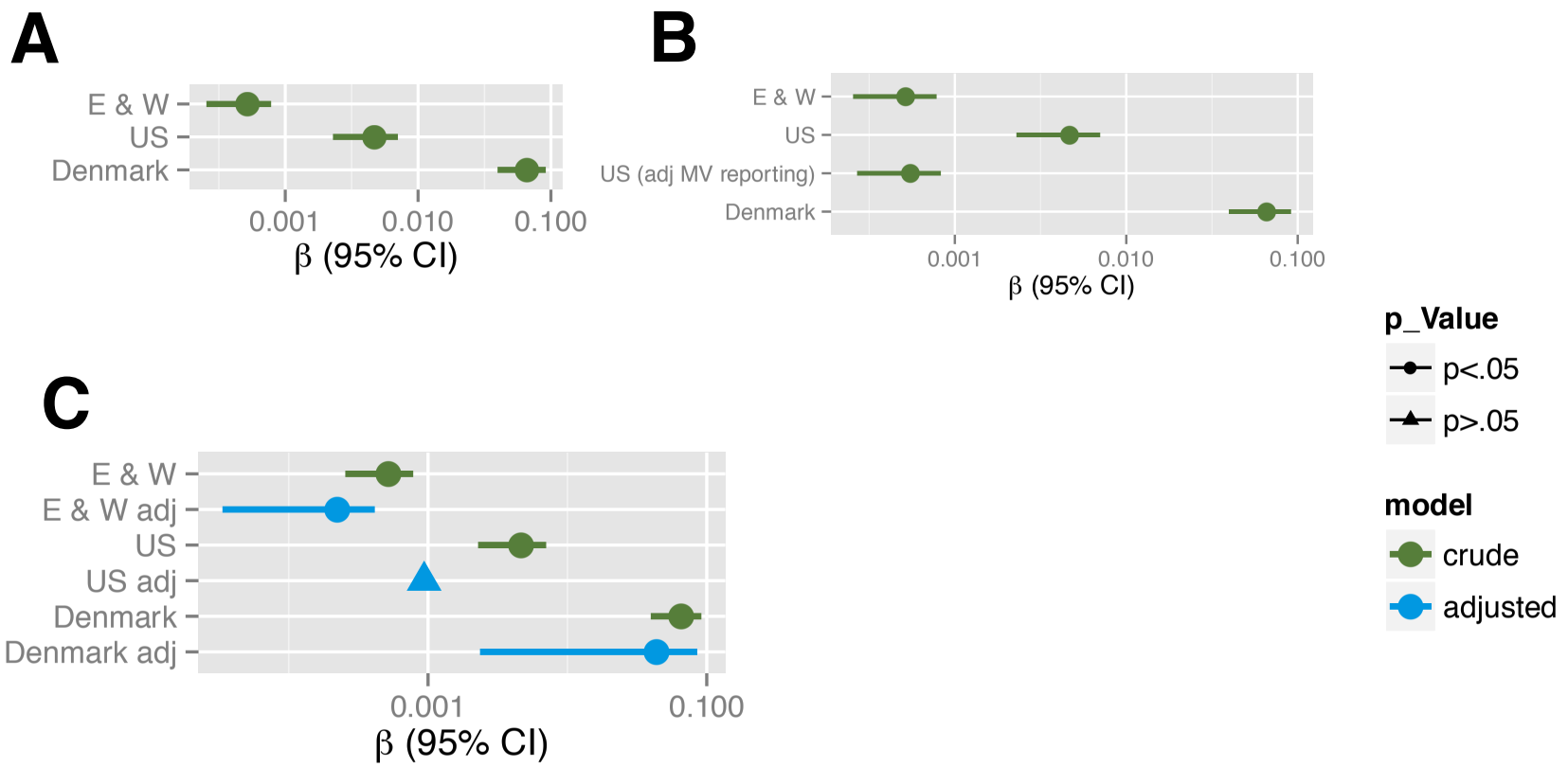

Figure S3: Coefficients of Association between non-measles infectious disease mortality and measles incidence. (A) Coefficients of association (β) for the regression of non-measles infectious disease mortality versus annual MV incidence for England and Wales, the US and Denmark. In **(B)** the coefficient of association is also shown for the US after adjusting the measles incidence data for significant underreporting, as discussed by Hinman, Orenstein and Papania (28). **(C)** Adjusting for year in the model had no effect on the point estimates of the regression coefficients, suggesting that adjusting for year does not significantly alter the relationship between measles and non-measles mortality.

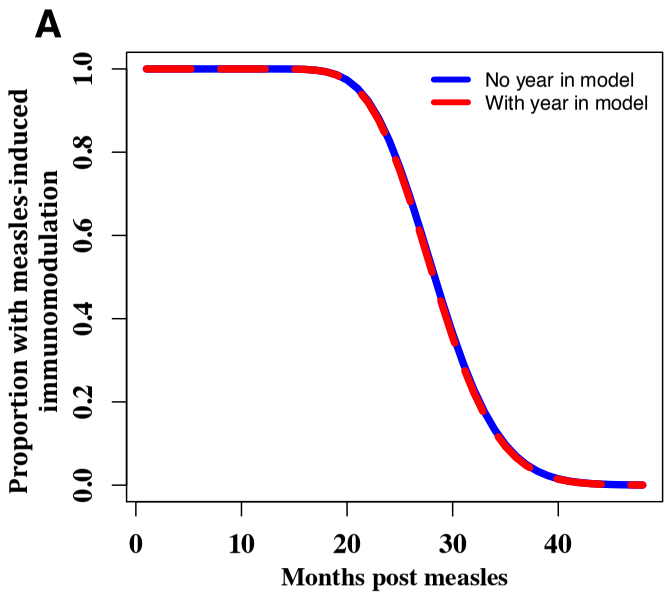

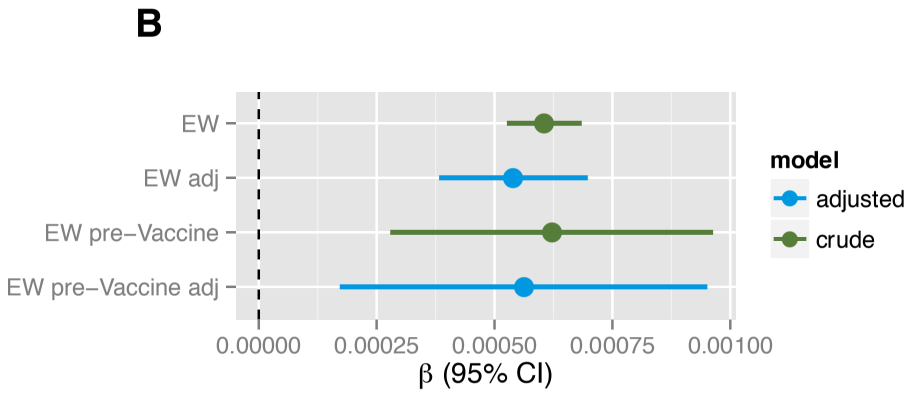

C

Years	Model	Predictor	β	P-value
All data	Crude	Immunomodulation	**6.07×10^{-4}**	**<.00001**
	Adjusted for year	Immunomodulation	**5.42×10^{-4}**	**<.00001**
		year	-4.19×10^{-2}	0.334
Pre-vaccine	Crude	immunomodulation	**6.21×10^{-4}**	**0.00163**
	Adjusted for year	immunomodulation	**5.616×10^{-4}**	**0.00825**
		year	3.85×10^{-2}	0.465

Figure S4: England & Wales: Adjusting for year has no effect on the relationship between measles immunomodulation and non-measles infectious disease mortality. (A) When year was included in the regression model to determine the best gamma-distribution, the best-fit distribution (ie: the gamma distribution that led to immunomodulation data with the best linear fit to the mortality data) was unchanged from the best-fit determined by regressing non-MV mortality against measles immunomodulation without including year as a covariate. **(B)** As well, at the best-fit gamma transformations, the regression coefficients were almost the same for both the full data set as well as for the pre-vaccine era analysis regardless of whether year was (adjusted) or was not (crude) added into the model as a covariate, and, shown in **(C)**, the regression coefficient for year was insignificant in both the analysis of the full data set as well as the pre-vaccine data analysis (p=0.334 and p=0.465, respectively). It can also be seen from both **(B)** and **(C)** that the regression coefficients, indicating the relationship between non-MV mortality and measles immunomodulation was precisely the for the full data set (pre- and post-vaccination) and for the pre-vaccine era only (crude: 6.07x10-4 vs. 6.21x10-4, respectively; and adjusted: 5.42x10-4 vs. 5.62x10-4, for full and pre-vaccine era only, respectively).

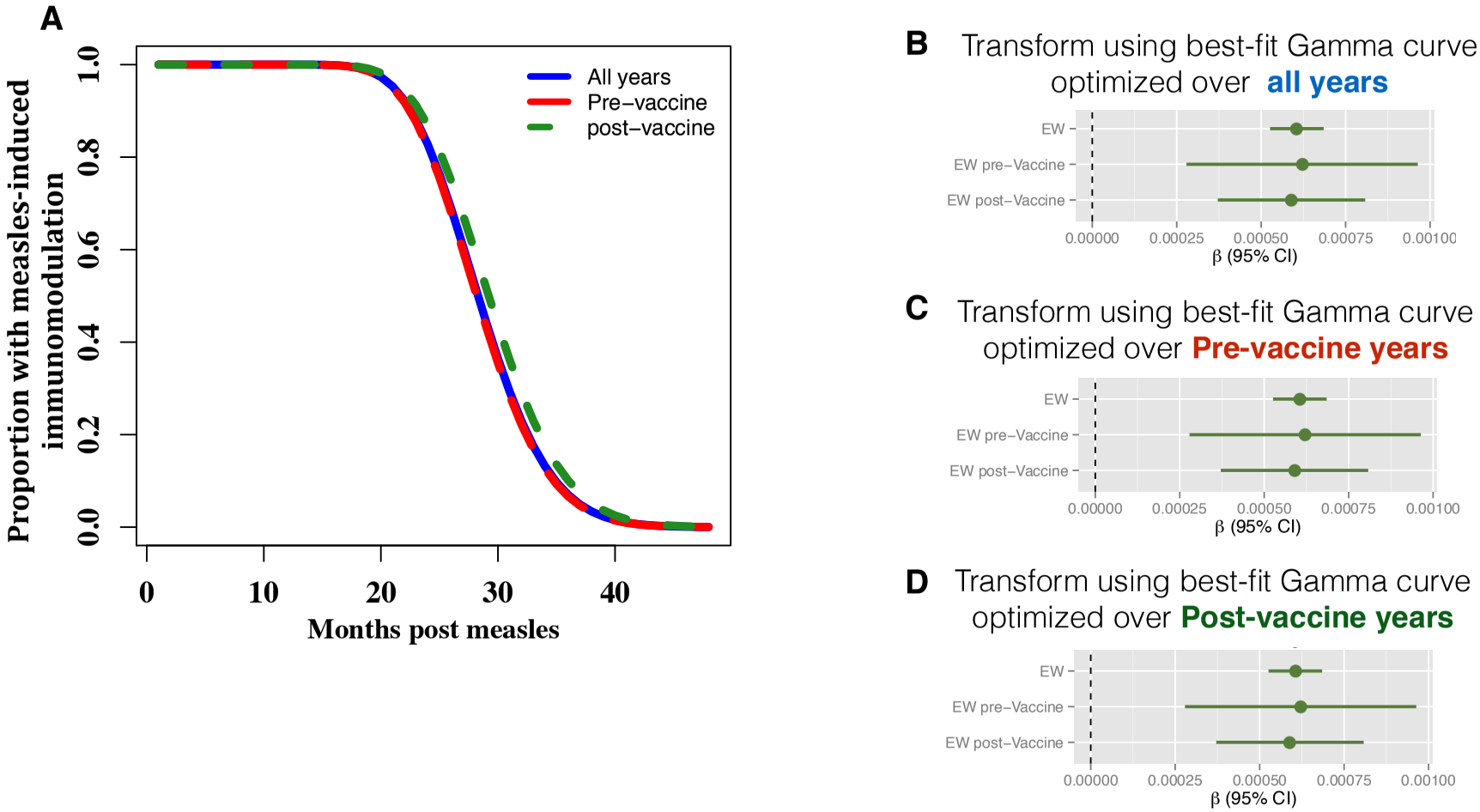

Figure S5: England & Wales Gamma Distribution and Regression Coefficients: (A) Best-fit gamma distributions when optimized over the full data set (blue), the pre-vaccine era (red) or the post-vaccine era (green). **(B-D)** the coefficients describing the relationship between non-MV mortality and measles immunomodulation were nearly identical between each of the eras (full data set, pre-vaccine era and post-vaccine era), and this held regardless of which era's best-fit gamma transform was used to transform the data. For example, in **(C)**, the gamma distribution was optimized while looking only at data collected during the pre-vaccine years, and, as shown in **(C)**, this optimized gamma distribution (red broken line in A) was used to transform: the full data set (EW), the pre-vaccine data (EW pre-Vaccine) and the post-vaccine measles incidence data (EW post-Vaccine) and then the the regression coefficients were calculated and are plotted in **(C)** with their 95% confidence intervals. The same is true for (B) and (D), except that in (B), the best-fit gamma transform used was optimized using the full data set and in **(D)**, the gamma transform was optimized using only the post-vaccine era data.

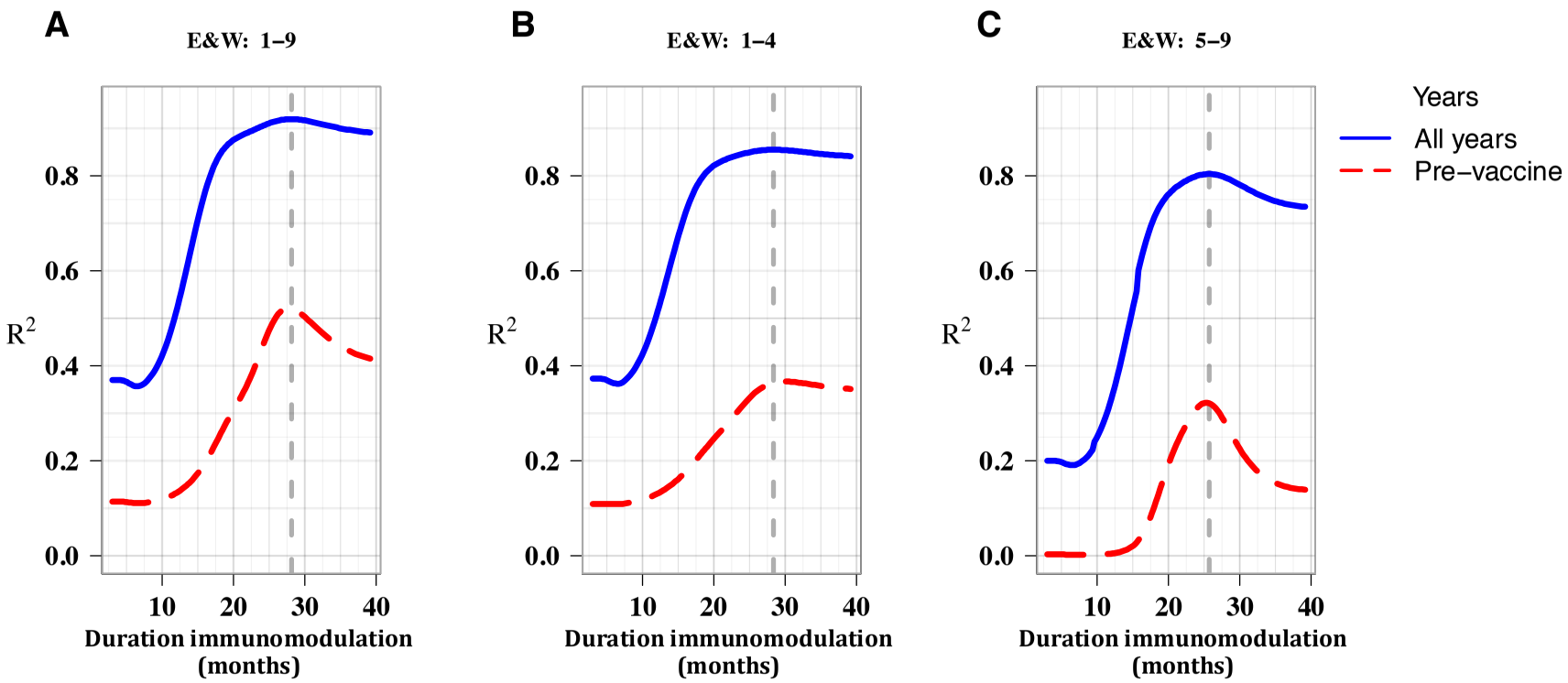

Figure S6: England & Wales: Optimum duration of immunomodulation is consistent across age groups. The R^2 versus duration of immunomodulation curves, as shown in Figure 2, are shown here for **(A)** 1-9 year olds (as in figure 2) **(B)** 1-4 year olds* and **(C)** 5-9 year olds* using the full data set (blue lines) or just the pre-vaccine-era data (red lines).

**Although measles incidence data was available for one- or two-year age groups for England & Wales, non-measles mortality data was available only for these more course age-groupings. Thus we were compelled to limit our analyses only to these more course age groupings. Nevertheless, the consistencies in the results between the age groupings (ie: 1-4 vs. 5-9) suggest strongly that having single-year age groupings would be unlikely to yield any different qualitative (and, for the most part, quantitative) results.*

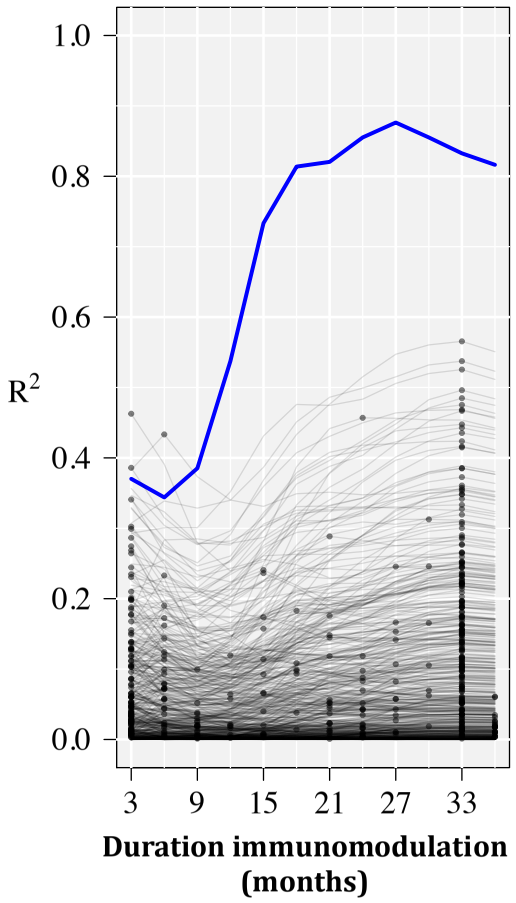

Figure S7: England & Wales: Randomizing by year removes improved fit with increasing duration of immunomodulation.

The full measles incidence data for England & Wales was transformed using the additive transform and the R^2 value for the linear regression of the non-measles infectious disease mortality versus the additively transformed data was plotted against the duration of immunomodulation (blue line; as shown in figure 2). To see if the large increase in linear-fit was specific to the order of the measles incidence data, each grey line represents a single simulation performed by first randomizing the E&W measles data by year (though order of individual quarters within years was preserved) and again applying the additive transform and plotting the R^2 value at each increase in duration of immunomodulation. The maximum R^2 value for each simulation is denoted by a filled point. This process was repeated over 200 simulations.

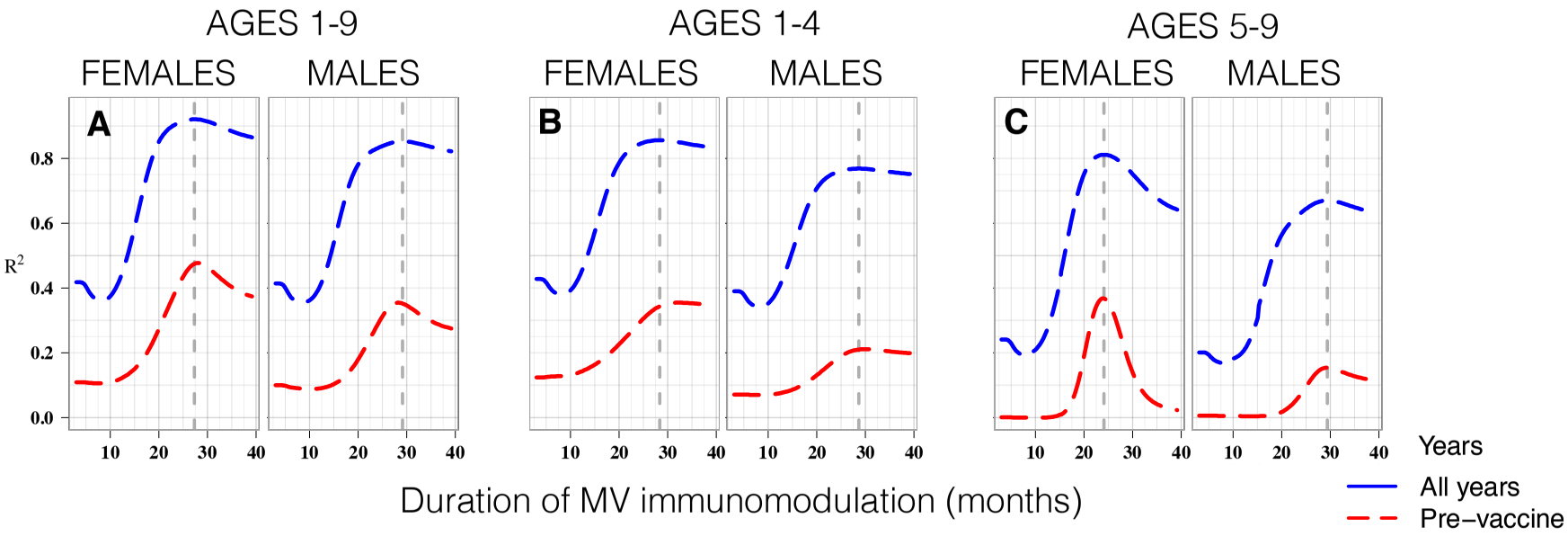

Figure S8: England & Wales: Association between non-measles mortality and measles-induced immunomodulation is stronger for females than males across age groups. The best-fit duration of immunomodulation was largely consistent between genders, regardless of age group (A: 1-9 years; B: 1-4 years; C: 5-9 years) and the overall fit and maximum fit of the non-measles infectious disease mortality to the measles immunomodulation was stronger for females than for males. This held whether observing over the full data set (blue lines) or the pre-vaccine data only (red lines).

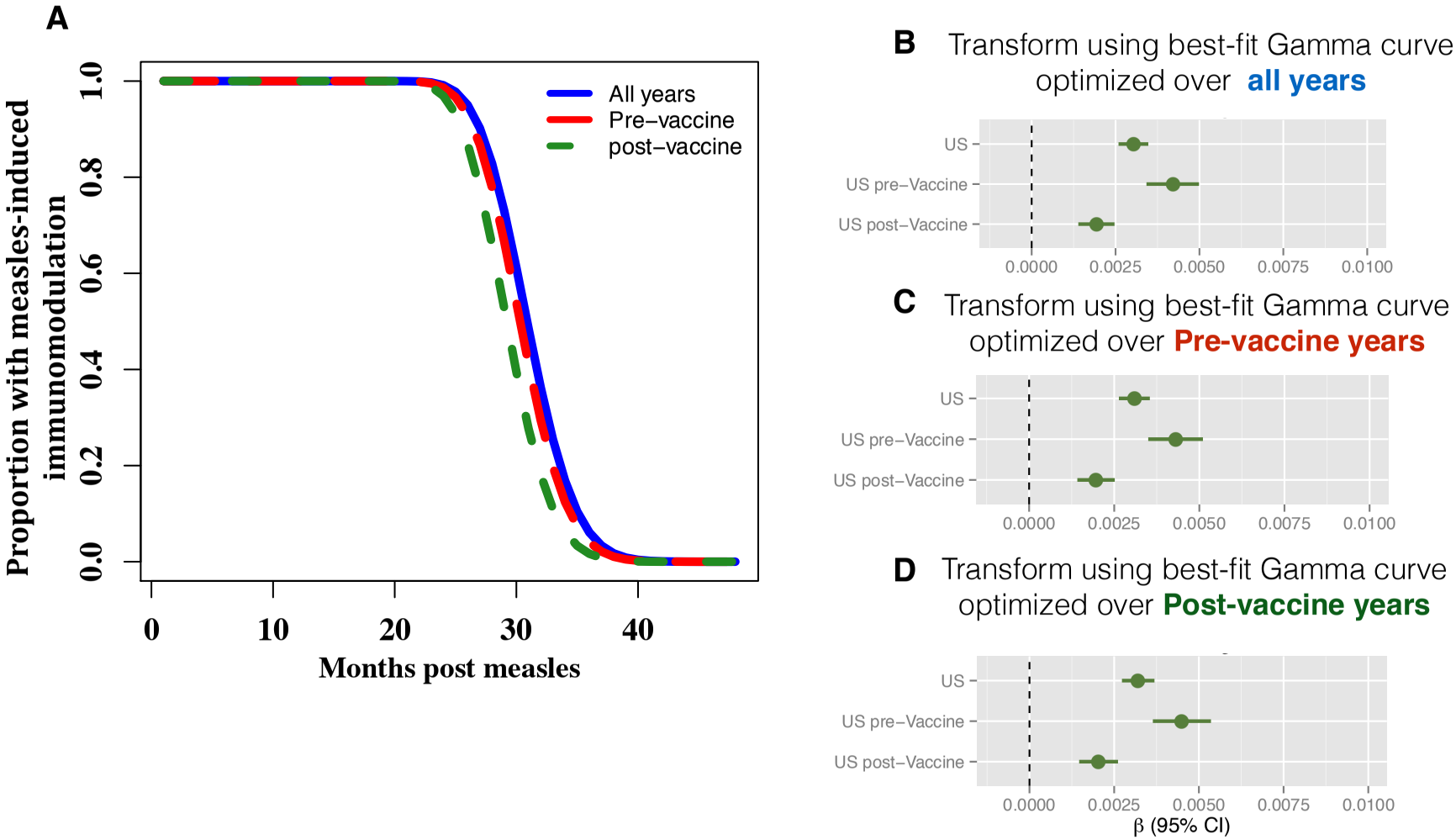

Figure S9: United States: Gamma Distribution and Regression Coefficients: (A) Best-fit gamma distributions when optimized over the full data set (blue), the pre-vaccine era (red) or the post-vaccine era (green). **(B-D)** the coefficients describing the relationship between non-MV mortality and measles immunomodulation were nearly identical between each of the eras (full data set, pre-vaccine era and post-vaccine era), and this held regardless of which era's best-fit gamma transform was used to transform the data. For example, in **(C)**, the gamma distribution was optimized while looking only at data collected during the pre-vaccine years, and, as shown in **(C)**, this optimized gamma distribution (red broken line in A) was used to transform: the full data set (US), the pre-vaccine data (US pre-Vaccine) and the post-vaccine measles incidence data (US post-Vaccine) and then the the regression coefficients were calculated and are plotted in **(C)** with their 95% confidence intervals. The same is true for (B) and (D), except that in (B), the best-fit gamma transform used was optimized using the full data set and in **(D)**, the gamma transform was optimized using only the post-vaccine era data.

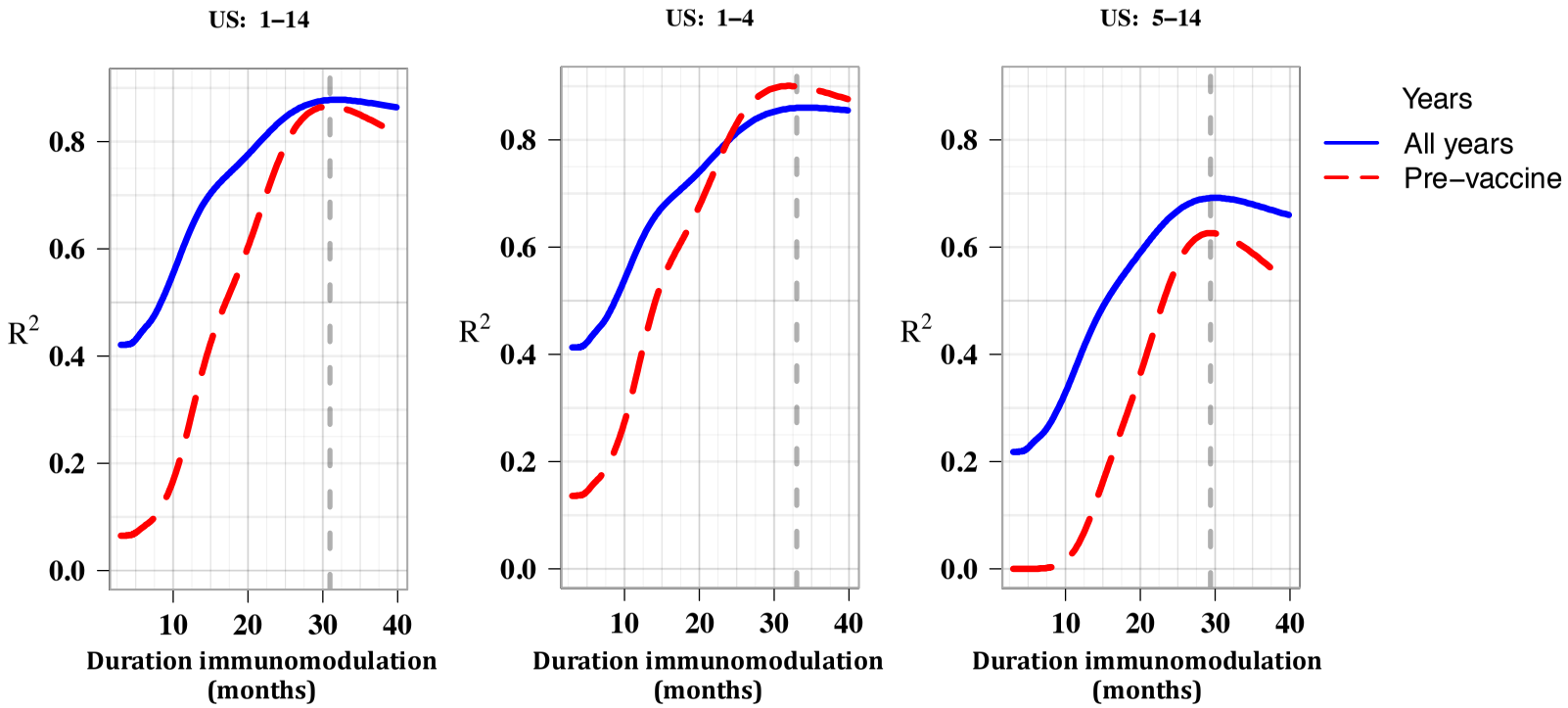

Figure S10: United States: Optimum duration of immunomodulation is consistent across age groups. The R^2 versus duration of immunomodulation curves, as shown in Figure 3, are shown here for **(A)** 1-14 year olds (as in figure 3) **(B)** 1-4 year olds* and **(C)** 5-14 year olds* using the full data set (blue lines) or just the pre-vaccine era data (red lines).

**Non-measles mortality data was available only for the course age-groupings listed above. Thus we were compelled to limit our subgroup analyses only to these more course age groupings (vs. one-year age groupings, for example). Nevertheless, the consistencies in the results between the age groupings (ie: 1-4 vs. 5-14) suggest strongly that having single-year age groupings would be unlikely to yield any different qualitative (and, for the most part, quantitative) results.*

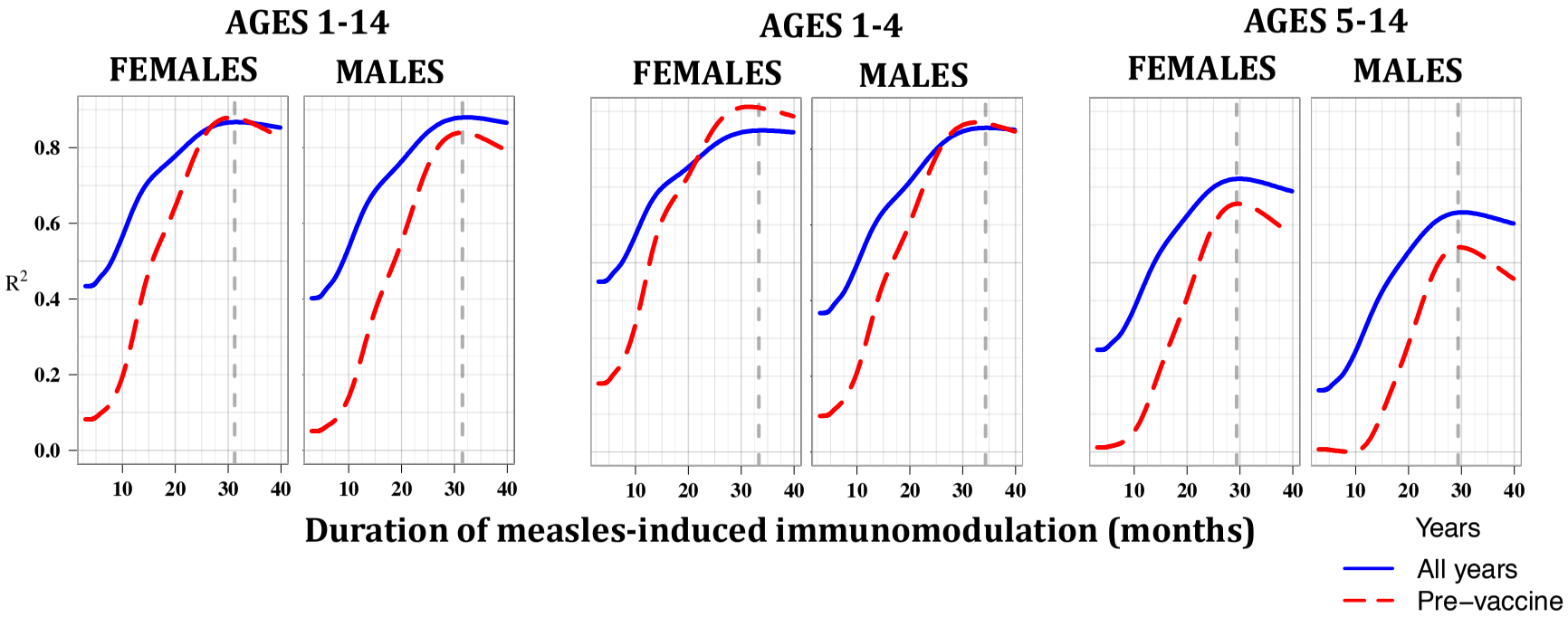

Figure S11: United States: Association between non-measles mortality and measles-induced immunomodulation is stronger for females than males across age groups. The best-fit duration of immunomodulation was largely consistent between genders, regardless of age group (A: 1-14 years; B: 1-4 years; C: 5-14 years) and the overall fit and maximum fit of the non-measles infectious disease mortality to the measles immunomodulation were stronger for females than for males. This held whether observing over the full data set (blue lines) or the pre-vaccine data only (red lines).

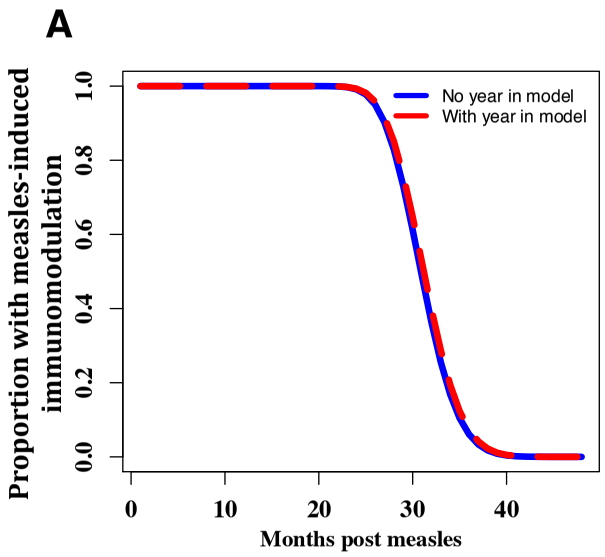

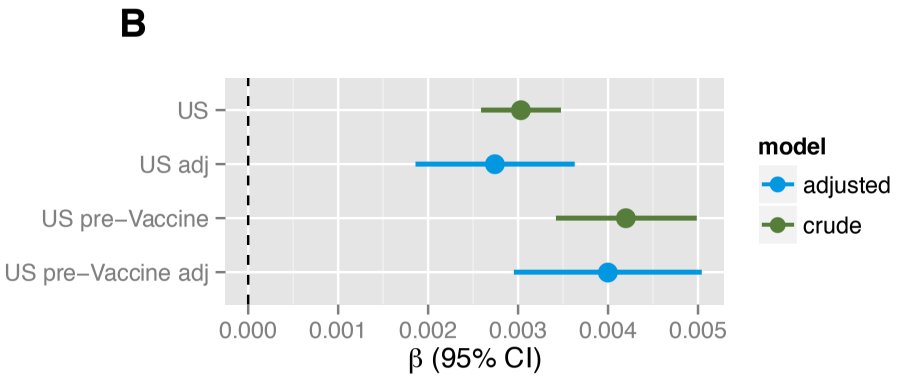

C

Years	Model	Predictor	β	P-value
All data	Crude	Immunomodulation	**3.03×10^{-3}**	**<0.00001**
	Adjusted for year	Immunomodulation	**2.74×10^{-3}**	**<0.00001**
		year	-3.59×10^{-2}	0.445
Pre-vaccine	Crude	immunomodulation	**4.20×10^{-3}**	**<0.00001**
	Adjusted for year	immunomodulation	**4.00×10^{-3}**	**<0.00001**
		year	2.86×10^{-2}	0.527

Figure S12: United States: Adjusting for year has no effect on the relationship between measles immunomodulation and non-measles infectious disease mortality. (A) When year was included in the regression model to determine the best gamma-distribution, the best-fit distribution (ie: the gamma distribution that led to immunomodulation data with the best linear fit to the mortality data) was unchanged from the best-fit determined by regressing non-MV mortality against measles immunomodulation without including year as a covariate. **(B)** As well, at the best-fit gamma transformations, the regression coefficients were almost the same for both the full data set as well as for the pre-vaccine era analysis regardless of whether year was (adjusted) or was not (crude) added into the model as a covariate, and, shown in **(C)**, the regression coefficient for year was insignificant in both the analysis of the full data set as well as the pre-vaccine data analysis (p=0.445 and p=0.527, respectively). It can also be seen from both **(B)** and **(C)** that the regression coefficients, indicating the relationship between non-MV mortality and measles immunomodulation was similar for the full data set and for the pre-vaccine era only.

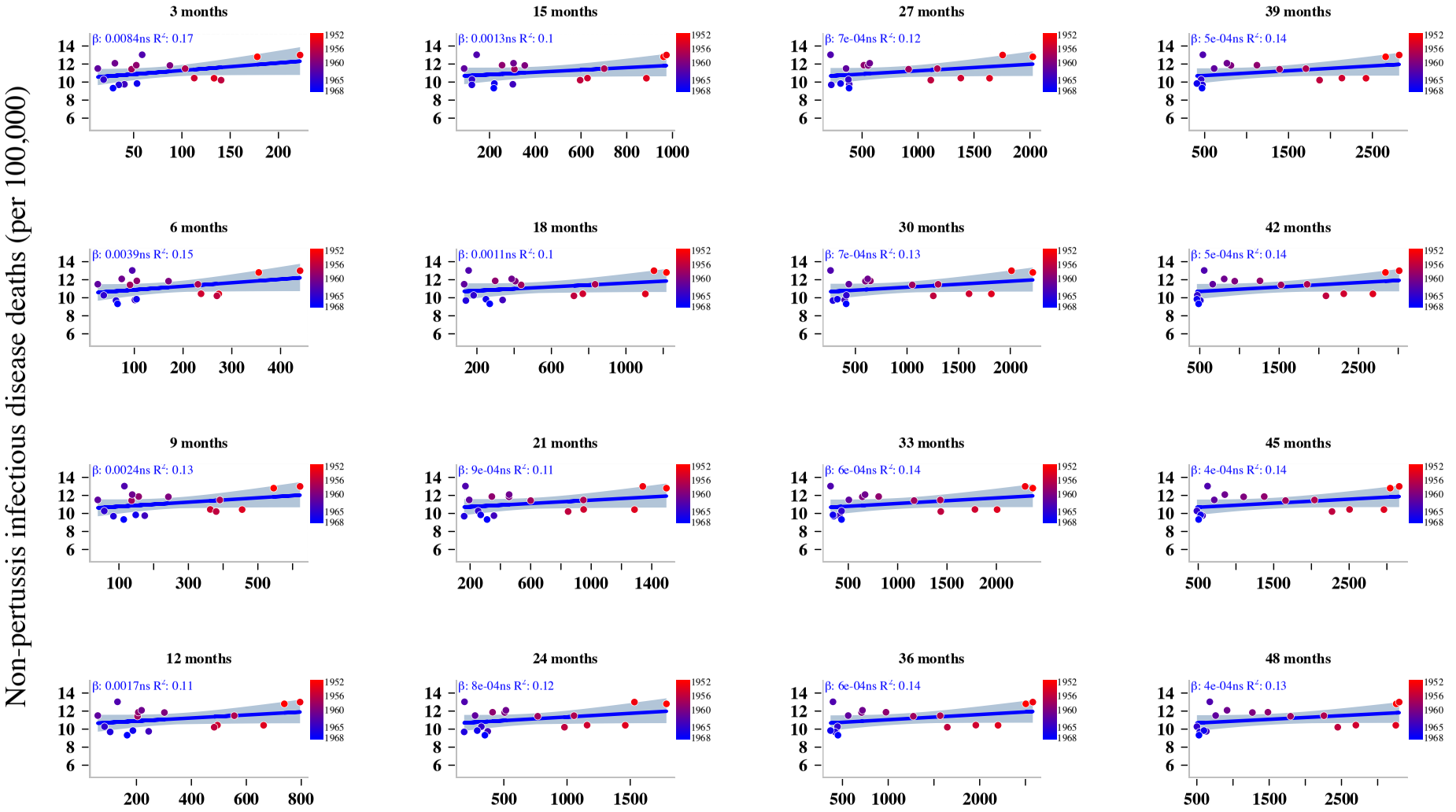

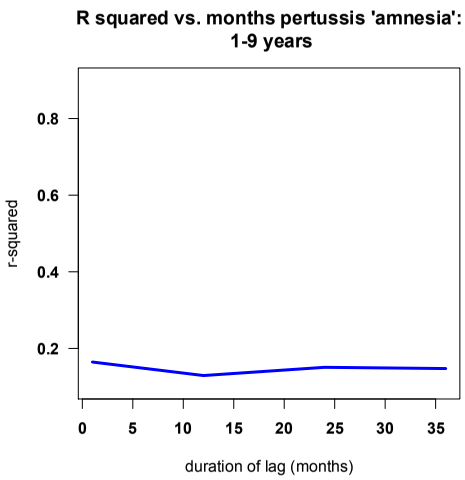

Figure S13: England & Wales: Relationship between pertussis and non-pertussis infectious disease mortality in the pre-measles vaccine era (1952-1968) in children 1-9 years of age. Based on high-quality weekly surveillance data.

Non-pertussis infectious disease mortality plotted against pertussis incidence (3 months) and plotted against pertussis with increasing durations over which cases were accumulated (6 months - 48 months; analogous to measles immunomodulation comprised of at-risk children accumulated over increasing durations of time from no lag (3 months) to 48 months. At bottom left: Correlation (R^2) between non-pertussis infectious disease mortality and accumulated pertussis cases plotted (per 100,000; from above) against the duration over which the cases were accumulated (as long as 48 months). Weekly pertussis data courtesy of Dr. Pejman Rohani and described in (34).

Cause of death	20th Century Mortality Files - 1940-1949 - ICD5	20th Century Mortality Files - 1950-1957 - ICD6	20th Century Mortality Files 1958-1967 - ICD7	20th Century Mortality Files 1968-1978 - ICD8
Atypical Pneumonia		4920	4920	
Dysentery & diarrhea	27a	0450,0 451, 0452, 0453, 0454	0450,0 451, 0452, 0453, 0454	0040, 0041, 0042, 0043, 0044, 0048, 0049
Bacteria	24d, 25, 26	0540, 0640, 0641, 0642, 0643, 0644	0540, 0630,	0390, 0391, 0399
Bacterial Pneumonia				4820, 4821, 4822, 4823, 4829
Bronchitis	106a, 106c	5000, 5010	5000, 5010	4660, 4900, 5180
Bronchopneumonia	107(1), 107(2)	4910	4910	4850
Brucellosis	5	0440	0440	0230, 0231, 0232, 0239
Cholera	4	0430	0430	0000, 0001, 0009
Dysentery	27b, 27c, 27d	0470, 0480	0470, 0480	0090, 0091, 0092, 0099
Encephalitis		0820, 0830, 0831, 0832, 0833	820, 821, 822, 823, 830, 831, 832, 833	
Fungal		1320, 1330, 1340, 1341, 1342, 1343, 1344, 1345	1340, 1341, 1342, 1343, 1344, 1345	1130, 1140, 1160-69, 1170-79
Lobar Pneumonia	108(1), 108(2)	4900	4900	
Meningitis	81	3400, 3401, 3402, 3403, 9440	3400, 3401, 3402, 3403	3200, 3201, 3208, 3209
Meningococcal Infection		0571, 0572, 0573	0571, 0572, 0573	0361, 0368, 0369
Otitis	89a	3900, 3910, 3911, 3912, 3920, 3921, 3922	3900, 3910, 3911, 3912, 3920, 3921, 3922	3800, 3810, 3811, 3819, 3820, 3821, 3829
Paratyphoid	2	0410	0410	0020, 0021, 0022, 0029
Plague	3	0580, 0581, 0582	0580, 0581, 0582	0200, 0201, 0209
Pneumococcal Pneumonia				4810
Pneumonia	109(1), 109(2)	4930	4930	4860
Respiratory	114e(2)			
Scarlet Fever	8			
Septicaemia	24a	0530, 0531, 0532, 0533, 0534	0530, 0531, 0532, 0533, 0534	0380, 0381, 0382, 0388, 0389
Streptococcal	115b(2)	0510	0510	0340, 0341
Typhoid	1	0400	0400	10
Other URT		4700, 4710, 4720, 4721, 4740, 4750	4700, 4710, 4720, 4721, 4730, 4740, 4750	4600, 4610, 4620, 4630, 4640, 4650
Varicella	38e	0870	0870	520
Viral Pneumonia				4800
Viruses	38f			

Table S1: England and Wales mortality data: Datasets and their respective International Classification of Disease (ICD) codes for E&W non-measles mortality data.

Movie S1: Example of Data Transformation: Measles Incidence to Measles Immunomodulation

Movie S2: Full Path of the England & Wales Gamma Transformation

Movie S3: Full Path of the USA Gamma Transformation

REFERENCES

1. W. J. Moss, D. E. Griffin, Measles. *Lancet* **379**, 153–164 (2012). Medline doi:10.1016/S0140-6736(10)62352-5

2. E. Simons, M. Ferrari, J. Fricks, K. Wannemuehler, A. Anand, A. Burton, P. Strebel, Assessment of the 2010 global measles mortality reduction goal: Results from a model of surveillance data. *Lancet* **379**, 2173–2178 (2012). Medline doi:10.1016/S0140-6736(12)60522-4

3. R. T. Perry, M. Gacic-Dobo, A. Dabbagh, M. N. Mulders, P. M. Strebel, J. M. Okwo-Bele, P. A. Rota, J. L. Goodson; Centers for Disease Control and Prevention (CDC), Global control and regional elimination of measles, 2000-2012. *MMWR Morb. Mortal. Wkly. Rep.* **63**, 103–107 (2014). Medline

4. S. B. Omer, D. A. Salmon, W. A. Orenstein, M. P. deHart, N. Halsey, Vaccine refusal, mandatory immunization, and the risks of vaccine-preventable diseases. *N. Engl. J. Med.* **360**, 1981–1988 (2009). Medline doi:10.1056/NEJMsa0806477

5. J. D. Clemens, B. F. Stanton, J. Chakraborty, S. Chowdhury, M. R. Rao, M. Ali, S. Zimicki, B. Wojtyniak, Measles vaccination and childhood mortality in rural Bangladesh. *Am. J. Epidemiol.* **128**, 1330–1339 (1988). Medline

6. M. A. Koenig, M. A. Khan, B. Wojtyniak, J. D. Clemens, J. Chakraborty, V. Fauveau, J. F. Phillips, J. Akbar, U. S. Barua, Impact of measles vaccination on childhood mortality in rural Bangladesh. *Bull. World Health Organ.* **68**, 441–447 (1990). Medline

7. A. Desgrées du Loû, G. Pison, P. Aaby, Role of immunizations in the recent decline in childhood mortality and the changes in the female/male mortality ratio in rural Senegal. *Am. J. Epidemiol.* **142**, 643–652 (1995). Medline

8. P. Aaby, J. Bukh, I. M. Lisse, A. J. Smits, Measles vaccination and reduction in child mortality: A community study from Guinea-Bissau. *J. Infect.* **8**, 13–21 (1984). Medline doi:10.1016/S0163-4453(84)93192-X

9. E. A. Holt, R. Boulos, N. A. Halsey, L. M. Boulos, C. Boulos, Childhood survival in Haiti: Protective effect of measles vaccination. *Pediatrics* **85**, 188–194 (1990). Medline

10. Z. Kabir, J. Long, V. P. Reddaiah, J. Kevany, S. K. Kapoor, Non-specific effect of measles vaccination on overall child mortality in an area of rural India with high vaccination coverage: A population-based case-control study. *Bull. World Health Organ.* **81**, 244–250 (2003). Medline

11. P. Aaby, T. R. Kollmann, C. S. Benn, Nonspecific effects of neonatal and infant vaccination: Public-health, immunological and conceptual challenges. *Nat. Immunol.* **15**, 895–899 (2014). Medline doi:10.1038/ni.2961

12. P. Aaby, A. Bhuiya, L. Nahar, K. Knudsen, A. de Francisco, M. Strong, The survival benefit of measles immunization may not be explained entirely by the prevention of measles disease: A community study from rural Bangladesh. *Int. J. Epidemiol.* **32**, 106–115 (2003). Medline doi:10.1093/ije/dyg005

13. K. L. Flanagan, R. van Crevel, N. Curtis, F. Shann, O. Levy; Optimmunize Network, Heterologous ("nonspecific") and sex-differential effects of vaccines: Epidemiology, clinical trials, and emerging immunologic mechanisms. *Clin. Infect. Dis.* **57**, 283–289 (2013). Medline doi:10.1093/cid/cit209

14. C. L. Karp, M. Wysocka, L. M. Wahl, J. M. Ahearn, P. J. Cuomo, B. Sherry, G. Trinchieri, D. E. Griffin, Mechanism of suppression of cell-mediated immunity by measles virus. *Science* **273**, 228–231 (1996). Medline doi:10.1126/science.273.5272.228

15. B. Hahm, Hostile communication of measles virus with host innate immunity and dendritic cells. *Curr. Top. Microbiol. Immunol.* **330**, 271–287 (2009). Medline doi:10.1007/978-3-540-70617-5_13

16. S. Schneider-Schaulies, J. Schneider-Schaulies, Measles virus-induced immunosuppression. *Curr. Top. Microbiol. Immunol.* **330**, 243–269 (2009). Medline doi:10.1007/978-3-540-70617-5_12

17. R. D. de Vries, S. McQuaid, G. van Amerongen, S. Yüksel, R. J. Verburgh, A. D. Osterhaus, W. P. Duprex, R. L. de Swart, Measles immune suppression: Lessons from the macaque model. *PLOS Pathog.* **8**, e1002885 (2012). Medline doi:10.1371/journal.ppat.1002885

18. J. Kleinnijenhuis, J. Quintin, F. Preijers, L. A. Joosten, D. C. Ifrim, S. Saeed, C. Jacobs, J. van Loenhout, D. de Jong, H. G. Stunnenberg, R. J. Xavier, J. W. van der Meer, R. van Crevel, M. G. Netea, Bacille Calmette-Guerin induces NOD2-dependent nonspecific protection from reinfection via epigenetic reprogramming of monocytes. *Proc. Natl. Acad. Sci. U.S.A.* **109**, 17537–17542 (2012). Medline doi:10.1073/pnas.1202870109

19. G. R. Lee, S. T. Kim, C. G. Spilianakis, P. E. Fields, R. A. Flavell, T helper cell differentiation: Regulation by cis elements and epigenetics. *Immunity* **24**, 369–379 (2006). Medline doi:10.1016/j.immuni.2006.03.007

20. M. G. Netea, J. Quintin, J. W. van der Meer, Trained immunity: A memory for innate host defense. *Cell Host Microbe* **9**, 355–361 (2011). Medline doi:10.1016/j.chom.2011.04.006

21. S. Saeed, J. Quintin, H. H. Kerstens, N. A. Rao, A. Aghajanirefah, F. Matarese, S. C. Cheng, J. Ratter, K. Berentsen, M. A. van der Ent, N. Sharifi, E. M. Janssen-Megens, M. Ter Huurne, A. Mandoli, T. van Schaik, A. Ng, F. Burden, K. Downes, M. Frontini, V. Kumar, E. J. Giamarellos-Bourboulis, W. H. Ouwehand, J. W. van der Meer, L. A. Joosten, C. Wijmenga, J. H. Martens, R. J. Xavier, C. Logie, M. G. Netea, H. G. Stunnenberg, Epigenetic programming of monocyte-to-macrophage differentiation and trained innate immunity. *Science* **345**, 1251086 (2014). Medline doi:10.1126/science.1251086

22. WHO, Meeting of the Strategic Advisory Group of Experts on immunization, March 2014, *Systematic Review of the Non-specific Effects of BCG, DTP and Measles Containing Vaccines*, http://www.who.int/immunization/sage/meetings/2014/april/3_NSE_Epidemiology_review_Report_to_SAGE_14_Mar_FINAL.pdf.

23. R. D. de Vries, R. L. de Swart, Measles immune suppression: Functional impairment or numbers game? *PLOS Pathog.* **10**, e1004482 (2014). Medline doi:10.1371/journal.ppat.1004482

24. W. H. Lin, R. D. Kouyos, R. J. Adams, B. T. Grenfell, D. E. Griffin, Prolonged persistence of measles virus RNA is characteristic of primary infection dynamics. *Proc. Natl. Acad. Sci. U.S.A.* **109**, 14989–14994 (2012). Medline doi:10.1073/pnas.1211138109

25. R. T. Perry, N. A. Halsey, The clinical significance of measles: A review. *J. Infect. Dis.* **189**, S4–S16 (2004). Medline doi:10.1086/377712

26. L. K. Selin, K. Vergilis, R. M. Welsh, S. R. Nahill, Reduction of otherwise remarkably stable virus-specific cytotoxic T lymphocyte memory by heterologous viral infections. *J. Exp. Med.* **183**, 2489–2499 (1996). Medline doi:10.1084/jem.183.6.2489

27. S. K. Kim, M. A. Brehm, R. M. Welsh, L. K. Selin, Dynamics of memory T cell proliferation under conditions of heterologous immunity and bystander stimulation. *J. Immunol.* **169**, 90–98 (2002). Medline doi:10.4049/jimmunol.169.1.90

28. S. K. Kim, R. M. Welsh, Comprehensive early and lasting loss of memory CD8 T cells and functional memory during acute and persistent viral infections. *J. Immunol.* **172**, 3139–3150 (2004). Medline doi:10.4049/jimmunol.172.5.3139

29. C. D. Peacock, S. K. Kim, R. M. Welsh, Attrition of virus-specific memory CD8+ T cells during reconstitution of lymphopenic environments. *J. Immunol.* **171**, 655–663 (2003). Medline doi:10.4049/jimmunol.171.2.655

30. A. R. Hinman, W. A. Orenstein, M. J. Papania, Evolution of measles elimination strategies in the United States. *J. Infect. Dis.* **189**, S17–S22 (2004). Medline doi:10.1086/377694

31. P. Aaby, J. Bukh, D. Kronborg, I. M. Lisse, M. C. da Silva, Delayed excess mortality after exposure to measles during the first six months of life. *Am. J. Epidemiol.* **132**, 211–219 (1990). Medline

32. WHO, *Global Review of the Distribution of Pneumococcal Invasive Disease by Age and Region* (2011); http://www.who.int/immunization/sage/6_Russel_review_age_specific_epidemiology_PCV_schedules_session_nov11.pdf.

33. O. Horwitz, K. Grünfeld, B. Lysgaard-Hansen, K. Kjeldsen, The epidemiology and natural history of measles in Denmark. *Am. J. Epidemiol.* **100**, 136–149 (1974). Medline

34. J. A. Clarkson, P. E. M. Fine, The efficiency of measles and pertussis notification in England and Wales. *Int. J. Epidemiol.* **14**, 153–168 (1985). Medline doi:10.1093/ije/14.1.153

35. A. Kipps, L. Stern, E. Vaughan, The duration and the possible significance of the depression of tuberculin sensitivity following measles. *S. Afr. Med. J.* **86**, 104–108 (1996).

36. S. O. Shaheen, P. Aaby, A. J. Hall, D. J. Barker, C. B. Heyes, A. W. Shiell, A. Goudiaby, Cell mediated immunity after measles in Guinea-Bissau: Historical cohort study. *BMJ* **313**, 969–974 (1996). Medline doi:10.1136/bmj.313.7063.969

37. S. O. Shaheen, P. Aaby, A. J. Hall, D. J. Barker, C. B. Heyes, A. W. Shiell, A. Goudiaby, Measles and atopy in Guinea-Bissau. *Lancet* **347**, 1792–1796 (1996). Medline doi:10.1016/S0140-6736(96)91617-7

38. P. Aaby, B. Samb, M. Andersen, F. Simondon, No long-term excess mortality after measles infection: A community study from Senegal. *Am. J. Epidemiol.* **143**, 1035–1041 (1996). Medline doi:10.1093/oxfordjournals.aje.a008667

39. P. Aaby, I. M. Lisse, K. Mølbak, K. Knudsen, H. Whittle, No persistent T lymphocyte immunosuppression or increased mortality after measles infection: A community study from Guinea-Bissau. *Pediatr. Infect. Dis. J.* **15**, 39–44 (1996). Medline doi:10.1097/00006454-199601000-00009

40. D. J. Earn, P. Rohani, B. M. Bolker, B. T. Grenfell, A simple model for complex dynamical transitions in epidemics. *Science* **287**, 667–670 (2000). Medline doi:10.1126/science.287.5453.667

41. B. T. Grenfell, R. M. Anderson, The estimation of age-related rates of infection from case notifications and serological data. *J. Hyg. London* **95**, 419–436 (1985). Medline doi:10.1017/S0022172400062859

42. J. Gindler, S. Tinker, L. Markowitz, W. Atkinson, L. Dales, M. J. Papania, Acute measles mortality in the United States, 1987-2002. *J. Infect. Dis.* **189**, S69–S77 (2004). Medline doi:10.1086/378565

43. W. G. van Panhuis, J. Grefenstette, S. Y. Jung, N. S. Chok, A. Cross, H. Eng, B. Y. Lee, V. Zadorozhny, S. Brown, D. Cummings, D. S. Burke, Contagious diseases in the United States from 1888 to the present. *N. Engl. J. Med.* **369**, 2152–2158 (2013). Medline doi:10.1056/NEJMms1215400